1-1-2005

Degradation of MgO Refractory in CaO-SiO2-MgO-FeOx and CaO-SiO2-Al2O3-MgO-FeOx Slags under Forced Convection

Sharon Nightingale
University of Wollongong, sharon@uow.edu.au

Geoff Brooks
Swinburne University of Technology

Brian J. Monaghan
University of Wollongong, monaghan@uow.edu.au

Degradation of MgO Refractory in $CaO-SiO_2-MgO-FeO_x$ and $CaO-SiO_2-Al_2O_3-MgO-FeO_x$ Slags Under Forced Convection

S.A. NIGHTINGALE, G.A. BROOKS, and B.J. MONAGHAN

Experiments based on exposure of MgO to slags under forced convection flow conditions allowed the identification of different degradation mechanisms and the assessment of the role of Al_2O_3 in the degradation process. Slag with no alumina present resulted in direct dissolution. Samples immersed in alumina containing slag underwent indirect dissolution, with a spinel forming at the MgO-slag interface. At 1530 °C, the spinel was not effective in reducing the corrosion rate, as the scattered spinel grains were easily removed from the MgO surface. At 1500 °C, the loss of MgO was reduced due to the formation of a more cohesive spinel layer. Mechanical erosion then appears to play a greater role. Strength of the bond between the spinel and underlying MgO needs to be considered in strategies to reduce degradation of MgO refractories.

I. INTRODUCTION

TWO of the key drivers in steelmaking operations are operational security and cost reduction. Steelmaking processes rely on refractory linings to contain the hot liquids and gases involved in producing steel. Modern processes increasingly use higher temperatures and techniques such as bottom bubbling and injection that greatly increase the flow of fluids within the vessel. These conditions are highly beneficial to productivity and can increase product quality. However, they also tend to significantly accelerate the rate of degradation of the refractory lining. Higher costs associated with more frequent replacement of the refractories and the associated down time are counterproductive, and some of the benefits of the new processing methods can be lost. Accelerated wear can also reduce product quality through an increase in the number of nonmetallic inclusions in the metal. Therefore, refractory performance has a significant impact on both operational security and costs.

Refractory materials based on magnesium oxide (MgO) are widely used to contain the molten metal, slag, and hot gases in steel processing vessels. However, much is still unknown about the fundamental interactions of molten steel, slag, and MgO refractories, which lead to corrosion, or about how changes in processing conditions affect corrosion and wear, particularly where there are flowing liquids or reaction products involved.

Studies of MgO immersed in molten slags under static conditions have found that a dense spinel ($MgO \cdot Al_2O_3$) or magnesiowustite ((Mg, Fe)O) layer formed at the MgO surface, significantly slowing the further dissolution of MgO.[1–5] The formation of these layers involves the counterdiffusion of ions, and is at least in part controlled by mass transfer. Layer thickness depends on the relative rates of growth of the solid solution (ss) at the MgO/ss interface and the dissolution of the ss at the ss/liquid interface. Goto *et al.*[6] performed cup tests on $MgO/MgO-Al_2O_3$ spinel refractories using a $CaO-SiO_2-Al_2O_3$ slag. They found that the spinel grain was subject to congruent dissolution, but the MgO dissolved incongruently, resulting in the formation of secondary spinel a short distance away from the refractory/slag interface. They postulated that this occurred because there was insufficient concentration of Al_2O_3 at the interface due to localized enrichment with MgO. More recent studies of MgO dissolution have also reported that the solid solution layer either formed at a distance from the solid surface, or initially formed there and then became detached and moved out into the liquid slag.[7,8] Under these conditions, this layer could be easily removed by forced liquid flow.

Sridhar and co-workers[9,10] used confocal scanning laser microscopy to directly observe the dissolution of small MgO particles in calcium silica aluminate[9] and calcium aluminate[10] slags at temperatures ranging from 1450 °C to 1600 °C. Convection effects were ignored. In these two studies, they reported conflicting rate controlling mechanisms for the MgO dissolution process. In the calcium silica aluminate[9] slag, it was concluded that boundary layer diffusion may be rate controlling, whereas in the calcium aluminate[10] slag, it was found that chemical reaction is rate limiting. Sridhar *et al.*[9,10] make no comment on the different rate controlling mechanisms. This difference may be due to changes in slag composition. In the calcium silica aluminate[9] study, they found evidence of spinel formation on the MgO particle as it dissolved.

Studies of dissolution under dynamic conditions have focused on alumina-based materials in contact with a variety of slag types. Such studies are complicated by the presence of three types of flow: interfacial flow caused by surface tension gradients at the solid/liquid/gas interface, density driven vertical flow caused by changes in composition of the slag at the solid/liquid interface, and forced convection flow. Masking of sections of the sample may be used to isolate one type of flow. For forced convection flow, it has been reported that the direct dissolution* of alumina in slag was controlled by mass transport across a boundary layer, as indicated by the dissolution rate being related to the square root of angular velocity.[11,12] Dunkl and Bruckner report that corrosion for a range of refractories exposed to $SiO_2-Al_2O_3-CaO-Na_2O$

*Direct dissolution is dissolution that takes place without formation of an intermediate dissolution product.

S.A. NIGHTINGALE and B.J. MONAGHAN, Senior Lecturers, are with the Faculty of Engineering, University of Wollongong, Wollongong, NSW, Australia 2522. Contact e-mail: sharon_nightingale@uow.edu.au G.A. BROOKS, Principal Research Scientist, CSIRO Minerals, Clayton South, VIC, Australia 3169.

Manuscript submitted May 24, 2004.

melts is initially nonlinear, and that vertical density flow must be overcome before forced convection dominates. They have also compiled results for all three types of flow, and determined effective diffusion coefficients, and concluded that interfacial convection flow has the greatest effect on corrosion.[13]

Indirect dissolution* of single-crystal alumina in CaO-MgO-Al_2O_3-SiO_2 melts has been studied by Sandhage and Yurek.[14,15,16] Spinel was formed both at 1450 °C and 1550 °C, with varying slag compositions and rotation speeds of 0 to 1400 rpm. With slag containing 10 pct MgO, the spinel layer was attached to the alumina only at infrequent points, with slag trapped between the sapphire and the spinel. At higher MgO contents, a complete spinel layer was formed at the interface that remained at a constant thickness over time. They concluded that even with forced convection flow, a steady state was quickly reached where the rate of spinel formation was equal to its rate of dissolution in the melt. Solid-state diffusion through the solid spinel layer and liquid-phase diffusion through the boundary layers were the rate controlling processes for spinel formation and dissolution. However, similar studies of the dissolution of MgO refractories in slag have not been reported.

*Indirect dissolution is a dissolution process in which a solid product forms.

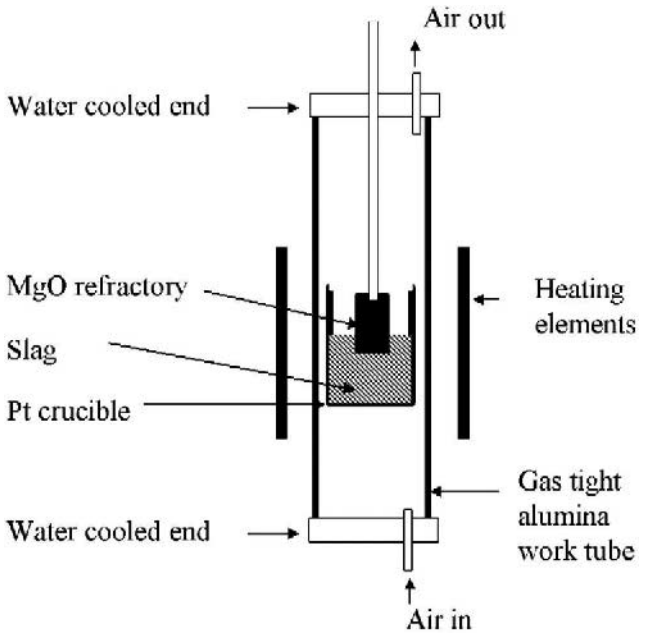

Fig. 1—Experimental set up for rotating finger corrosion tests.

Mukai *et al.*[17] have used *in-situ* X-ray observation techniques to study the penetration of porous MgO by a range of CaO-SiO_2-Al_2O_3-Fe_tO slags. Slag penetrated the pore networks, dissolving MgO. Al_2O_3 reacted with MgO to form spinel, and the resultant volume expansion restricted further slag ingress and restricted penetration. It is clear that much has still to be done to gain a complete understanding of MgO dissolution in steelmaking slags. Of particular significance is the location and conditions under which the protective spinel layer forms.

Therefore, the specific aims of this investigation are as follows.

(1) Firstly, to study the corrosion mechanisms involved in the degradation of MgO refractory in CaO-SiO_2-FeO_x-MgO and CaO-SiO_2-FeO_x-MgO-Al_2O_3 melts under conditions of forced convection flow, with a particular focus on the formation of a solid solution layer and its role in preventing corrosion.
(2) Secondly, to investigate the effects of slag composition, temperature, and liquid flow rates on the degradation process.

II. EXPERIMENTAL METHOD

A series of experiments was developed to study the effect of slag composition, temperature, and liquid flow on the degradation of MgO in steelmaking slags under highly controlled conditions. Of particular interest were the roles of alumina and forced convection flow on the degradation process.

A rotating finger apparatus (RFA) was used to carry out the experiments, as shown in Figure 1. The samples were heated in a dry air (industrial grade) atmosphere, and the temperature was monitored using a type B Pt/Rh thermocouple. The RFA was computer controlled and could rotate the sample at speeds of up to 800 rpm. The furnace had a hot zone of ±2 °C over 50 mm. A gas flow rate of 150 ml/min was used throughout the experiments.

A matrix of experiments was devised totaling 28 distinct experimental conditions. The conditions of each experiment are summarized in Table I.

Table I. Experimental Conditions

Slag A						Slag B					
T = 1530 °C											
Speed (rpm)	15 min	30 min	45 min	60 min	90 min	Speed (rpm)	15 min	30 min	45 min	60 min	90 min
50	•					50	•				
200	•					200	•				
400	•					400	•				
600	•					600	•				
800	•	•	•	•	•	800	•	•	•	•	•
T = 1500 °C											
Speed (rpm)						Speed (rpm)					
600	•					600	•				
800	•		•		•	800	•	•		•	•

Table II. Slag Compositions (Weight Percent)

	CaO	SiO_2	MgO	Al_2O_3	Fe_2O_3	FeO
Slag A	46	46	3.0	<0.1	4.3	0.8
Slag B	36	36	3.0	20	4.4	0.9

The slag compositions used are given in Table II. These compositions represent analysis of the fused slag material using an ARL (Fisons) 8680 SIM/SEQ XRF X-ray fluorescence apparatus (Rojan Advanced Ceramics, Henderson, West Australia). Analysis of FeO was performed using the potassium dichromate back titration method. These analysis techniques were also used to measure slag compositions at the end of the experiments.

Master slags were prepared by mixing the appropriate amounts of high-purity CaO, SiO_2, Al_2O_3, MgO, and Fe_2O_3 in a ball mill for a minimum of 8 hours before melting the mixture in a platinum crucible at 1550 °C in air using a muffle furnace. The master slags were then ground and remelted in the muffle furnace. This procedure was followed three times to produce a homogeneous slag. Separate chemical analyses of each batch of slag indicated that actual composition was within 4 pct of these values.

A slag basicity of 1 is similar to that at the beginning of the basic oxygen furnace (BOF) process when the slag has the greatest capacity to dissolve the refractory. The amount of alumina was selected to favor spinel formation

The cylindrical MgO test samples* (20-mm o.d. and 25 mm in length) were of high-purity MgO (>97 pct), and had a typical grain size of 20 to 50 μm and density of greater than 96 pct theoretical. Dense samples were selected to minimize the effects of pore penetration on the rate of MgO dissolution.

*Supplied by Rojan Advanced Ceramics, Henderson, Western Australia.

The refractory sample was positioned just above the crucible, and the furnace was heated to the experimental temperature at 10 °C/min, and held for 30 minutes to thermally equilibrate. The refractory sample was then lowered into the slag, and rotation commenced. After the required rotation time had elapsed, the rotation was stopped and the sample was immediately raised out of the furnace and water quenched.

The quenched samples were sectioned using a diamond wheel and cold mounted using epoxy resin. The samples were prepared for microscopy using standard grinding and polishing methods. The cross-sectional area of corroded samples was measured using digital image analysis techniques.

The corrosion rates of the samples were monitored by evaluating the changes in sample profile, cross-sectional area, and MgO concentration in the slag.

III. RESULTS

A. *Corrosion Profiles*

Corrosion profiles of the samples exposed to slag A were significantly affected by rotation speed. At 50 rpm, wear was fairly uniform and there was little slag line cutting. As rotation speed increased, slag line cutting became more pronounced, and wear at the bottom of the sample was also increased, resulting in a slightly conical shape. The effects of longer exposure times at 800 rpm were very pronounced with most corrosion occurring near the bottom end of the sample, as illustrated in Figure 2.

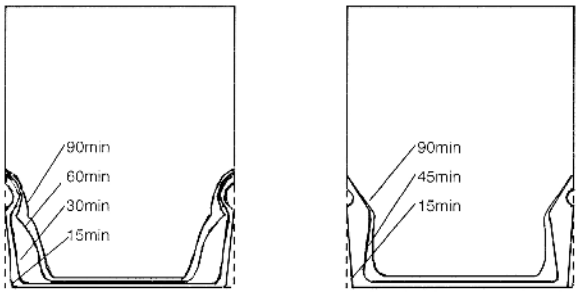

Fig. 2—Schematic diagram of sample profiles after exposure to Slag A at 800 rpm as a function of time. Left: 1530 °C after 15, 30, 60 and 90 min. Right: 1500 °C after 15, 45 and 90 min. Dashed lines indicate the original shape.

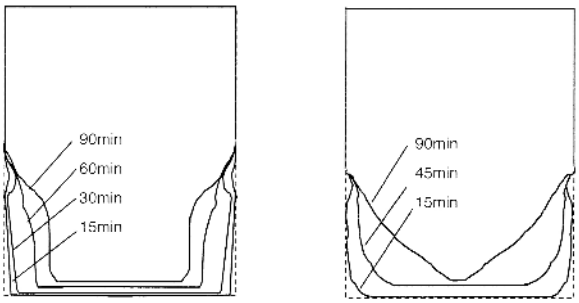

Fig. 3—Schematic diagram of sample profiles after exposure to Slag B at 800 rpm as a function of time. Left: 1530 °C after 15, 30, 60 and 90 min. Right: 1500 °C after 15, 45 and 90 min. Dashed line indicates original shape.

The profiles of the corroded samples tested with slag B at 1530 °C were similar in shape to those of slag A, but there was more material loss toward the bottom of the sample. Samples tested with slag B at 1500 °C suffered the greatest loss at the bottom, and developed a conical shape, as shown in Figure 3.

B. *Slag Composition*

Figure 4 shows how the MgO level in the bulk slag after 15 minutes varied as a function of rotation speed for both slags A and B at 1530 °C. Figure 5 shows the MgO level in the slag as a function of time for a fixed rotation speed (800 rpm) for both slags at two temperatures.

C. *Microstructural Observations*

Microstructural examination of samples exposed to Slag A (no Al_2O_3) showed that intergranular penetration was restricted to a narrow surface region approximately 20 to 100 μm in width. Even in the most corroded regions, the MgO surface remained quite smooth, as shown in Figure 6, indicating that there was no significant dislodging of MgO grains, even at 800 rpm. No solid reaction product was evident at the slag-MgO interface. Poorly formed crystalline phases were present in the solidified slag (possibly pseudowollastonite ($CaO{\cdot}SiO_2$) and merwinite ($3CaO{\cdot}MgO{\cdot}2SiO_2$)) as well as glass. It is likely that these phases formed during cooling.

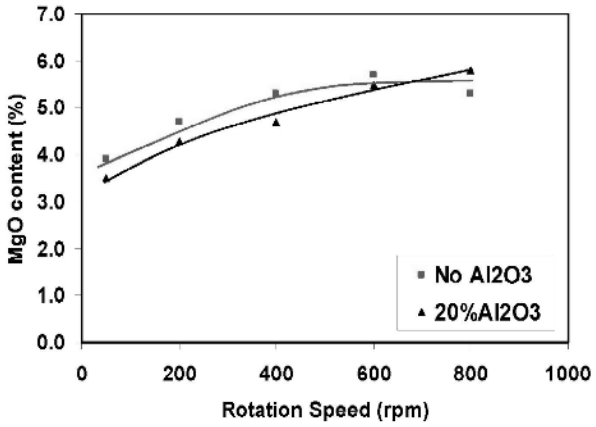

Fig. 4—MgO content of the slag after 15 min test at 1530 °C as a function of rotation speed for slag with and without alumina.

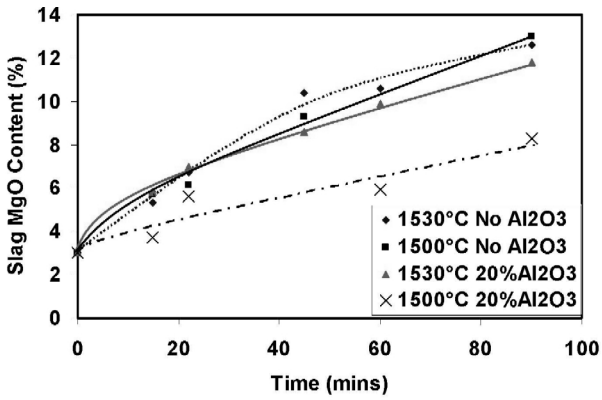

Fig. 5—MgO content of the slag after testing at 800 rpm as a function of time.

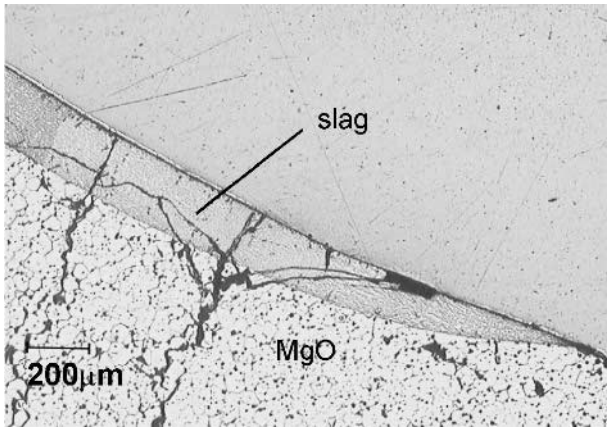

Fig. 6—Optical micrograph of Slag A-MgO interface after 90 min at 800 rpm, 1530 °C. (reflected light)

Microscopy of samples exposed to slag B showed that slag penetration was again restricted to a narrow region. A euhedral reaction product was formed at the interface, which displayed the cubic habit associated with a spinel. Energy-dispersive X-ray analysis confirmed that the phase is $MgO \cdot Al_2O_3$ with some iron oxide present in the solid solution.

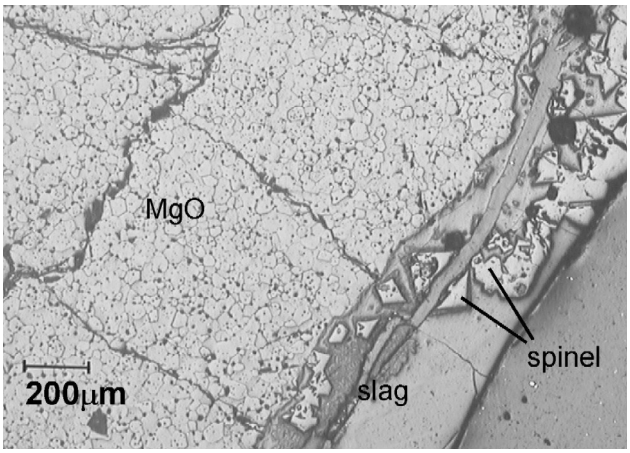

Fig. 7—Optical micrograph of Slag B-MgO interface after 90 min at 800 rpm, 1530 °C. (reflected light)

The spinel grains did not form a coherent layer, but were present as discrete grains either attached to the interface or near it. The number and size of spinel grains increased with exposure time and decreased temperature. At higher rotation speeds, the interface was quite rough, with spinel grains breaking off and moving out into the slag, as shown in Figure 7.

IV. DISCUSSION

From the sample profiles, it is clear that liquid flow has a major effect on degradation of the submerged samples. Increased flow can both accelerate chemical interactions and cause mechanical wear. The characteristic "coning" and rough interfaces observed for the samples tested in slag B indicate that grains of refractory weakened by corrosion break preferentially from the weakest mechanical point of the sample as it is spinning. This means that erosion/corrosion profiles formed, in part, reflect the mechanical aspects of how a spinning cylinder interacts with a fluid. The sample profiles also show that surface tension driven flow at the liquid/solid/gas interface contributes to corrosion. This effect has been discussed elsewhere.[18]

If the dissolution of the MgO was at least in part controlled by mass transfer in the slag phase, it would be expected that the dissolution rate would be a function of slag flow velocity, which is, in turn, a function of sample rotation speed. If chemical reaction or diffusional transport in the solid phase were rate controlling, and mechanical wear of the solid was not significant, then the dissolution rate would be independent of the slag flow velocity and sample rotation speed.

The results presented in Figure 4 indicate that the rate of degradation for slag A in the first 15 minutes increased with rotation speed up to about 600 rpm, after which the rate seems to have reached a plateau. This suggests that the corrosion rate is becoming insensitive to fluid flow rate. Therefore, it is likely that for slag A, the reaction is at least in part controlled by mass transfer in the slag phase at speeds up to about 600 rpm, when chemical reaction rate or diffu-

sional transport in the solid phase control becomes dominant. A graph of corrosion rate *vs* the square root of angular rotation speed, as opposed to the direct correlation given in Figure 4, shows a similar relationship.

The rate of degradation for slag B (20 pct Al_2O_3) in the first 15 minutes continued to increase with rotation speeds above 600 rpm, unlike the results obtained for slag A. This indicates that mass transfer is still, in part, rate controlling. However, this result could be affected by mechanical erosion.

The change in MgO content over time at 800 rpm shown in Figure 5 suggests that for slag A, the rate of degradation is approximately proportional with time (approximately 0.1 wt pct MgO/min) and that lowering the temperature to 1500 °C has very little effect on the reaction rate. The results for slag B at 800 rpm and 1530 °C are also proportional with time (approximately 0.1 wt pct MgO/min at 1530 °C), which is consistent with the results obtained for slag A. However, lowering the temperature to 1500 °C did have a significant effect on the reaction rate, almost halving the rate of MgO pick up in this slag.

To assess and quantify the kinetics of the MgO dissolution process, rate constants (k) were calculated using the chemical analyses of the slag, the measured surface area of the sample at the end of the experiment, and the volume of slag using the following integrated first-order rate equation:

$$-\ln\left[\frac{(C_{eq}-C_f)}{(C_{eq}-C_i)}\right] = k\frac{At}{V} \qquad [1]$$

where

V = volume of slag,
t = time,
A = interfacial area,
C_{eq} = concentration of MgO at the interface (assumed to equal saturation value),
C_f = final concentration of MgO in the slag, and
C_i = initial concentration of MgO.

Both slags had a lime:silica ratio of 1 and a starting MgO composition of 3.0 wt pct. Calculations performed using MTDATA* indicate that slag A will have a saturation MgO content of 21.2 pct at 1530 °C and 20.8 pct at 1500 °C. The phase diagram is shown in Figure 8. Slag B had an alumina content of 20 wt pct. Results from MTDATA calculations indicate that this slag will have a saturation MgO content of 20.3 pct at 1530 °C and 14.6 pct at 1500 °C. The phase diagram is shown in Figure 9.

Results for the 800 rpm experiments are shown in Figure 10 and Table III.

There is no significant difference between the rate constants for the two slags at 1530 °C. However, at 1500 °C, k is reduced by half for slag B. This is discussed in the section

*MTDATA[19] is a commercial thermodynamic software package developed at the National Physical Laboratory in the United Kingdom, which is able to calculate complex multicomponent phase equilibria in gas-liquid-solid systems. It uses a Gibbs energy minimization routine to establish the thermodynamic equilibrium of a defined system.

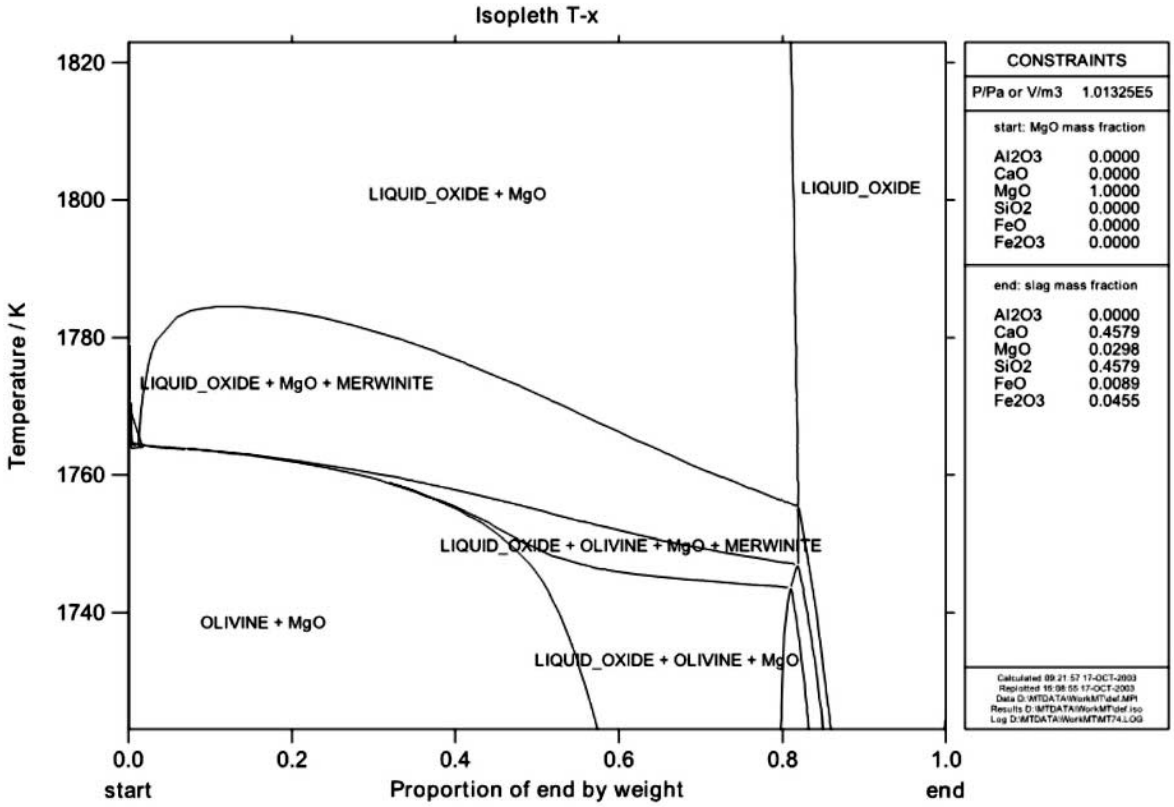

Fig. 8—Equilibrium phase stability for the MgO-Slag A system. "Start" is 100% MgO, and "End" is 100% Slag A. Due to the scale used in this diagram, the MgO phase field at the MgO rich end of the diagram cannot be resolved.

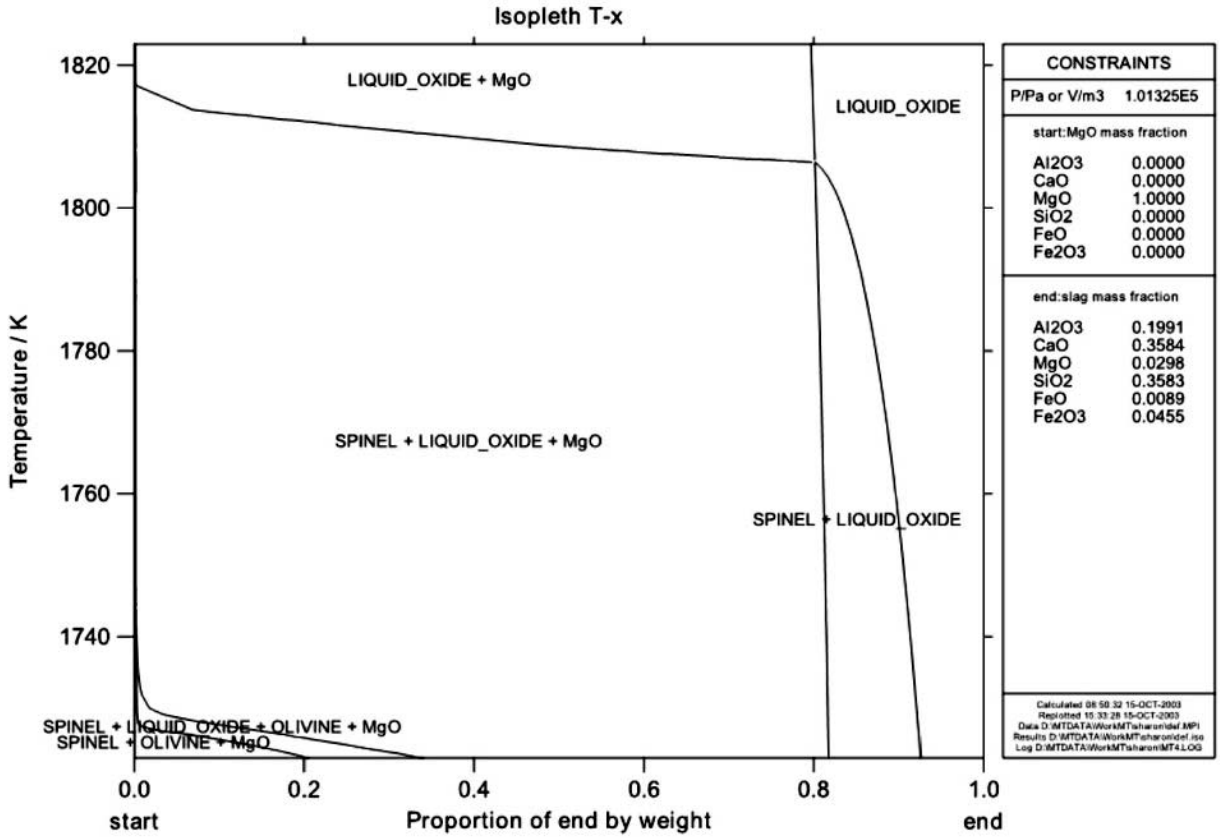

Fig. 9—Equilibrium phase stability for the MgO-Slag B system. "Start" is 100% MgO, and "End" is 100% Slag B. Due to the scale used in this diagram, the MgO phase field at the MgO rich end of the diagram cannot be resolved.

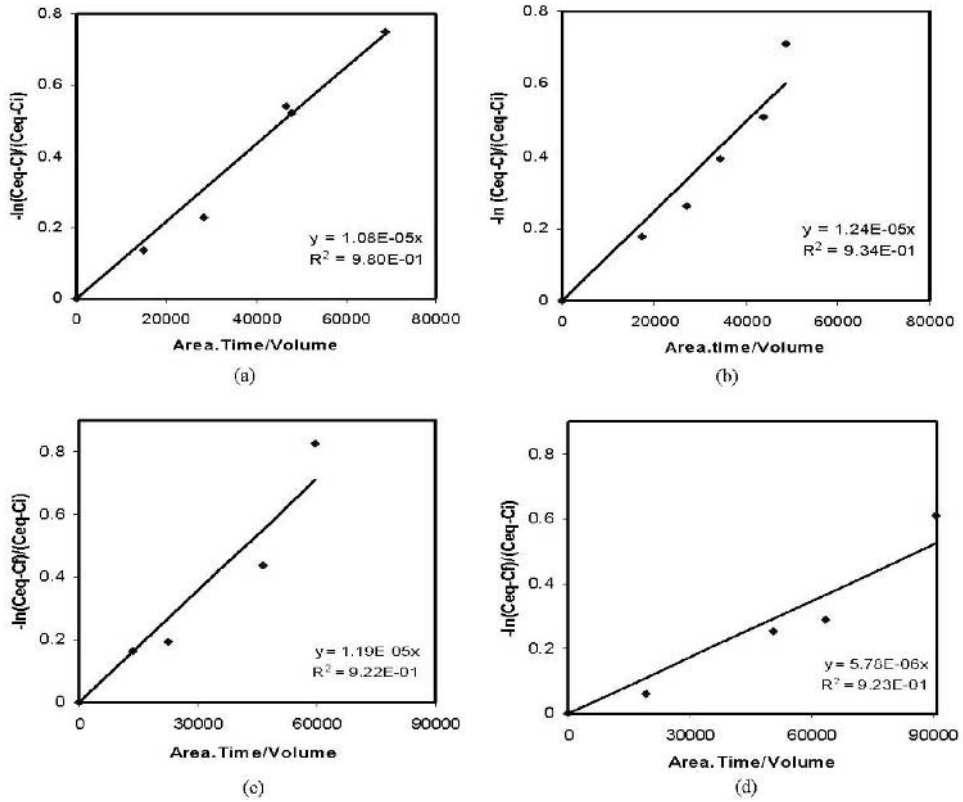

Fig. 10—First order rate constants at 800 rpm (*a*) Slag A at 1530 °C (*b*) Slag B at 1530 °C (*c*) Slag A at 1500 °C (*d*) Slag B at 1500 °C.

on spinel formation. Rate constants as a function of rotation speed are shown in Figure 11.

In Figure 11, it can be seen that the calculated first-order rate constant for both slags increases with increasing sample rotation speed. This is consistent with mass transfer in the slag phase being in part rate controlling, and is further evidence in support of this controlling mechanism. The plateau in rate constant at rotation speeds greater than 600 rpm (Figure 11(a)) for slag A is indicative that the rate controlling mechanism is no longer limited by mass transfer but by chemical reaction at the interface.

Effect of Spinel Formation on the Rate of Dissolution of MgO

The compositions of slags A and B were chosen to discriminate the effects of spinel formation on the dissolution kinetics. On the assumption that there is no kinetic impediment to the phases being formed, Figures 8 and 9 show that at 1500 °C and 1530 °C, the spinel would be expected to form as an intermediate dissolution product in slag B but not slag A. Microscopy of samples from this investigation (Figures 6 and 7) confirm the formation of a spinel product in slag B but not A. This is consistent with what other workers have observed.[14,15,16]

It is reasonable to expect that MgO refractory-slag systems where spinel forms during the dissolution of the refractory would have a different dissolution rate and rate constant from systems where no spinel forms. This is what other authors have argued,[14,15,16] who have shown that spinel slows the rate of refractory dissolution. What is most interesting about experiments at 1530 °C and 800 rpm for slag with alumina is that the overall rate is very similar to slag without alumina, indicating that any spinel formed does not provide significant protection to the MgO.

The different effects of temperature on the dissolution rate of the samples in alumina containing slag B compared to slag A are also interesting. In the case of slag B (20 pct Al_2O_3), the overall rate is strongly reduced by lowering the temperature from only 1530 °C to 1500 °C, whereas lowering the temperature in the slag A experiments had little effect. These results can be explained by considering the effects of temperature on the phase stability of the system and the nature of the spinel layer formation. Given the small temperature difference in these experiments, and the scatter within the data, it is not unexpected that one rate constant could be used to represent the MgO dissolution data, as found for slag A (Table III). What is more surprising is the approximately 50 pct decrease in the value of k for slag B over this temperature range. This is indicative of a significant change in the dissolution mechanism. There was also a significant change in the observed sample profile (Figure 3) that suggests there was a greater degree of mechanical erosion of the MgO sample using slag B at 1500 °C. This change in wear characteristic could be responsible for the change in kinetics.

As shown in Figure 9, the saturation level for MgO in slag B changes rapidly with temperature in this range. At 1500 °C, substantially less MgO must dissolve before spinel precipitation commences, and further dissolution is inhibited. Micrographs confirm that more spinel is present at the lower temperature and that it forms a more cohesive layer than at 1530 °C, as shown in Figure 12.

After 15 minutes at 1530 °C and 600 rpm, there are some scattered spinel grains either attached to or near the interface. After the same amount of time, but at 1500 °C, there is extensive spinel formation, but the layer is attached to the MgO at infrequent intervals. It is not clear whether the spinel has been undermined by slag penetration or, as proposed by Sandhage and Yurek,[14] it nucleates at the MgO refractory surface, and then grows sideways, trapping slag between the spinel and the MgO. At the higher temperature, more MgO dissolves before spinel precipitation occurs and the growth of spinel is faster. This faster growth of the spinel is likely to lead to a weaker bond with the MgO substrate making it easier to be sheared from the refractory and removed to the slag. In Figure 13, a micrograph of the refractory-slag system after 90 minutes at 1530 °C and 800 rpm, there is evidence of the spinel having been sheared from the refractory. In this figure, some large spinel grains can be seen in the slag at a distance from the interface containing remnant MgO particles. Other spinels were observed attached to the MgO surface. The most probable location for the formation

Table III. First-Order Rate Constants ($m \cdot s^{-1}$) for 800 rpm Experiments

Slag Type	1530 °C	1500 °C
Slag A—no Al_2O_3	1.1×10^{-5}	1.2×10^{-5}
Slag B—20 pct Al_2O_3	1.2×10^{-5}	0.58×10^{-5}

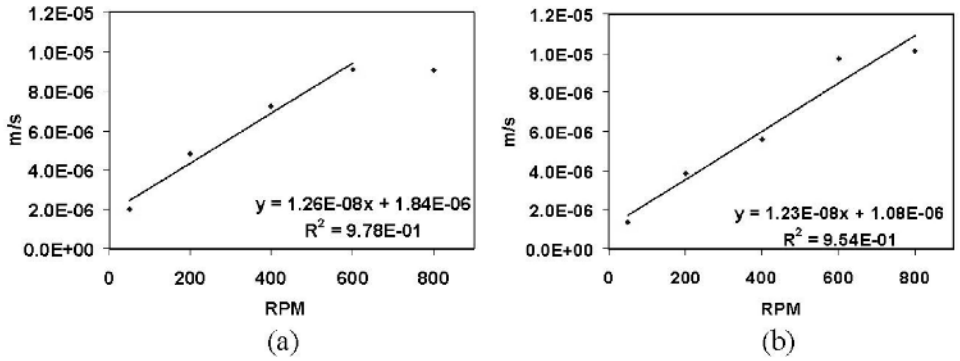

Fig. 11—First order rate constants as a function of sample rotation speed after 15 min at 1530 ºC. (*a*) Slag A (*b*) Slag B.

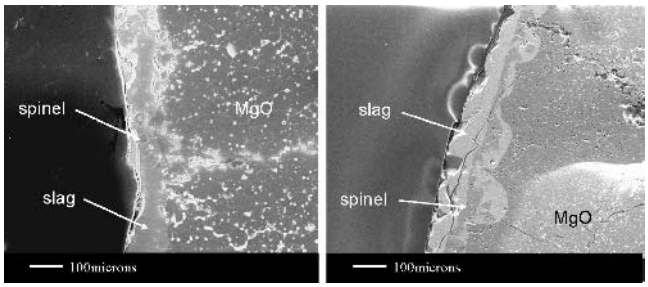

Fig. 12—Spinel formation at (*a*) 1530 °C and at (*b*) 1500 °C, 600 rpm after 15 minutes. Cracks in the samples are due to quenching.

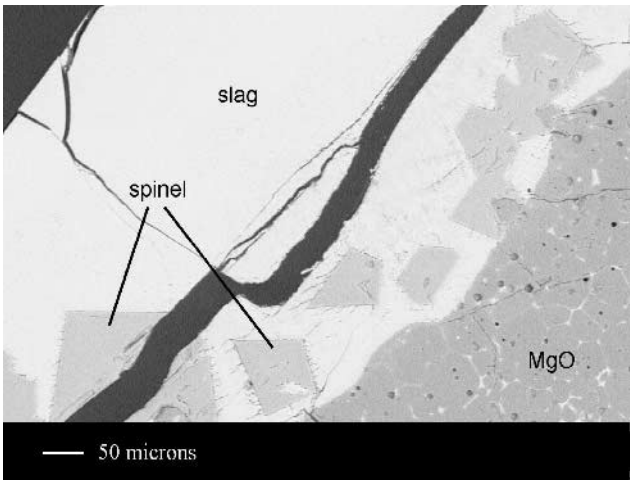

Fig. 13—Spinel grains located near the MgO surface, some containing remnant MgO particles (dark grey), and some forming a small bridge connected to the MgO. Slag B, 90 min at 1530 °C and 800 rpm.

of these isolated spinel grains at a distance from the interface is on the surface of the MgO.

Whether the spinel remains attached to the refractory or is sheared off into the slag will have a significant bearing on the rate of the refractory dissolution. If the spinel is removed, then "fresh" refractory will be exposed to the dissolving slag. Until this spinel reforms, the refractory is essentially unprotected. This is the probable explanation of why there is such a difference in the rate constants calculated for the different temperatures using slag B.

The conical profile and ragged interfaces of the samples tested in slag B as compared to slag A (Figures 2, 3, 6, and 7) suggest that spinel formation may actually make the MgO more likely to suffer mechanical damage in situations where the refractory is subject to high liquid flow rates and associated high shear forces. The periphery would be exposed to a greater liquid flow rate than the central axis, which would magnify these effects. The spinels appear to nucleate and grow at small protrusions on the MgO surface. These protrusions could easily be broken, and the spinel detached from the surface, exposing a fresh MgO surface to the slag. Formation of a continuous, coherent layer well bonded to the surface is needed to provide an effective barrier to dissolution.

Overall, for the slag compositions and conditions studied, the dissolution of the refractory can be described by a single equation relating k and rotation speed unless a coherent spinel layer is formed. This has important consequences for developing strategies for refractory corrosion minimization in liquid metal processing, as it demonstrates that a complete description of the dissolution process requires not only knowledge of the thermodynamics, diffusion, and fluid flow of the system, but will also have to incorporate the strength of the bond between the spinel layer and the underlying MgO.

V. CONCLUSIONS

1. In nonalumina bearing slag, MgO underwent direct dissolution. The rates of corrosion were consistent with a first-order kinetic process. Mass transfer was at least in part rate controlling up to a rotation speed of 600 rpm, beyond which chemical reaction rate control appears dominant.
2. In alumina bearing slag, MgO underwent indirect dissolution, with spinel forming as a reaction product. The rates of corrosion were consistent with a first-order kinetic process. Mass transfer was at least in part rate controlling at all sample rotation speeds tested. A change to reaction rate control may have been masked by mechanical erosion.
3. Spinel initially formed at the slag/MgO interface, and was then subsequently detached. There was no evidence to support formation of spinel in the bulk slag away from the interface.
4. At 1530 °C, under forced convection conditions, formation of spinel did not reduce the rate of degradation of MgO, as the isolated grains were easily dislodged.
5. At 1500 °C, spinel did slow degradation as a result of formation of a reasonably coherent layer.
6. Even at 1500 °C, the spinel layer is only attached at intermittent locations by narrow MgO protrusions. Therefore, at high flow rates, shear stresses may lead to fracture, loss of spinel layer, and accelerated degradation.
7. The strength of the bond between the spinel and the underlying MgO needs to be included in strategies for minimization of MgO dissolution during steelmaking.

ACKNOWLEDGMENTS

The authors thank Lee Brunckhorst, Ahmed Mosbah, and Kevin Matsunaga, for their assistance with this project. We also thank the Australian Research Council, BHP Research, and BlueScope Steel for their financial support.

REFERENCES

1. J. Bygden, T. DebRoy, and S. Seetharaman: *Ironmaking and Steelmaking*, 1994, vol. 21 (4), pp. 318-23.
2. N. Allen, S. Sun, and S. Jahanshahi: *2nd Melt Chemistry Symp*., Melbourne, Australia, CSIRO Division of Minerals, Clayton, Victoria, Australia, 1995, pp. 55-59.
3. P. Zhang and S. Seetharaman: *J. Am. Ceram. Soc*., 1994, vol. 77 (4), pp. 970-76.
4. M. Wallace, S. Sun, and S. Jahanshahi: *6th AusIMM Extractive Metallurgy Conf*., Brisbane, Australia, AusImm, Carlton South, Victoria, Australia, 1994, pp. 37-40.
5. P. Vadasz and L. Molnar: *Ceram.-Silikaty*, 1992, vol. 36, pp. 199-204.
6. K. Goto, B.B. Argent, and W.E. Lee: *J. Am. Ceram. Soc*., 1997, vol. 80 (2), pp. 461-71.

7. R. Rait: Ph.D. Thesis, University of Melbourne, Melbourne, 1997.
8. T. Tran, S. Nightingale, and G. Brooks: *J. Aust. Ceram. Soc*., 1998, vol. 34 (2), pp. 33-38.
9. M. Valdez, K. Prapakorn, A.W. Cramb, and S. Sridhar: *Steel Res*., 2001, vol. 72, pp. 291-97.
10. K.W. Yi, C. Tse, J.-H. Park, M. Valdez, A.W. Cramb, and S. Sridhar: *Scand. J. Metall*., 2003, vol. 32, pp. 177-84.
11. A.R. Cooper and W.D. Kingery: *J. Am. Ceram. Soc*., 1964, vol. 47 (1), pp. 37-43.
12. M. Dunkl and R. Bruckner: *Glastech Ber*., 1987, vol. 60 (8), pp. 261-67.
13. M. Dunkl and R. Bruckner: *Glastech Ber*., 1989, vol. 62 (1), pp. 10-19.
14. K.H. Sandhage and G.J. Yurek: *J. Am. Ceram. Soc*., 1988, vol. 71 (6), pp. 478-89.
15. K.H. Sandhage and G.J. Yurek: *J. Am. Ceram. Soc*., 1990, vol. 73 (12), pp. 3633-42.
16. K.H. Sandhage and G.J. Yurek: *J. Am. Ceram. Soc*., 1990, vol. 73 (12), pp. 3643-49.
17. K. Mukai, A. Tao, K. Goto, Z. Li, and T. Takashima: *Proc. 6th Int. Conf. on Molten Slags, Fluxes and Salts*, June 2000, CD by Trita Met. 85, paper 69.
18. Y. Chen, G. Brooks, S. Nightingale, K. Coley, and M. Hamed: *Advances in Refractories for the Metallurgical Industries IV*, 4th Int. Symp., Canadian Institute of Mining, Metallurgy, and Petroleum, Montreal, Canada, 2004, pp. 513-26.
19. R.H. Davies, A.T. Dinsdale, J.A. Gisby, S.M. Hodson, and R.G.J. Ball: *Conf. on Applications Thermodynamics on the Synthesis and Processing of Materials*, ASM/TMS, Rosemont, IL, 1994, pp. 371-84.